



Nonlinear Dynamics and Strong Cavity Cooling of Levitated Nanoparticles

P. Z. G. Fonseca, E. B. Aranas, J. Millen, T. S. Monteiro, and P. F. Barker*

Department of Physics and Astronomy, University College London, Gower Street, London WC1E 6BT, United Kingdom

(Received 21 December 2015; published 21 October 2016)

Optomechanical systems explore and exploit the coupling between light and the mechanical motion of macroscopic matter. A nonlinear coupling offers rich new physics, in both quantum and classical regimes. We investigate a dynamic, as opposed to the usually studied static, nonlinear optomechanical system, comprising a nanosphere levitated in a hybrid electro-optical trap. The cavity offers readout of both linear-in-position and quadratic-in-position (nonlinear) light-matter coupling, while simultaneously cooling the nanosphere, for indefinite periods of time and in high vacuum. We observe the cooling dynamics via both linear and nonlinear coupling. As the background gas pressure was lowered, we observed a greater than 1000-fold reduction in temperature before temperatures fell below readout sensitivity in the present setup. This Letter opens the way to strongly coupled quantum dynamics between a cavity and a nanoparticle largely decoupled from its environment.

DOI: [10.1103/PhysRevLett.117.173602](https://doi.org/10.1103/PhysRevLett.117.173602)

Cavity optomechanics, the cooling and coherent manipulation of mechanical oscillators using optical cavities, has undergone rapid progress in recent years [1], with many experimental milestones realized. These include cooling to the quantum level [2,3], optomechanically induced transparency (OMIT) [4], and the transduction [5–7] and squeezing [8] of light. These important processes are due to a linear light-matter interaction, linear in both the position of the oscillator \hat{x} and the amplitude of the optical field \hat{a} .

Nonlinear optomechanical interactions open up a new range of applications which are so far largely unexplored. In principle, they allow quantum nondemolition (QND) measurements of energy and, thus, the possibility of monitoring quantum jumps in a macroscopic system [1,9]. They also offer the prospect of observing phonon quantum shot noise [10], nonlinear OMIT [11,12], and the preparation of macroscopic nonclassical states [13]. To achieve a nonlinear interaction one can use optical means, which require strong single-photon coupling to the mechanical system [11,12] but are a considerable experimental challenge. Nonlinearities can also arise from spatial, mechanical effects, by engineering, for example, a light-matter interaction of the form $(\hat{a} + \hat{a}^\dagger)(G_1\hat{x} + G_2\hat{x}^2)$ where \hat{a} and \hat{a}^\dagger are the photon creation and annihilation operators, \hat{x} and \hat{x}^2 are the position and position squared operators, and G_1 and G_2 are the linear and nonlinear coupling between the field and the motion. Previous studies investigated the static shift in the cavity resonant frequency [9,14,15] or the quadratic optical spring effect [15] arising from a nonlinear coupling.

In this Letter, we study a nanosphere levitated in a hybrid system formed from a Paul trap and an optical cavity [16] as shown in Fig. 1. The output of the cavity is used to access the linear and nonlinear dynamics of the particle. We are able to tune the linear to nonlinear ratio ($G_1 : G_2$) to reach

$G_1 \sim 0$, isolating the true nonlinear dynamics. Further, due to the dynamic nature of this experiment, we are able to observe the damping, in time, of the cavity field modulations driven by the nonlinear coupling; to our knowledge, this has not been previously observed, and G_2 effects have not been previously detected in any levitated system. This is distinct from recently observed position-squared behavior, by control of the detection quadrature on resonance [17], in a system with purely linear G_1 coupling. These nonlinear dynamical effects are also unrelated to variations in mechanical oscillation frequency arising when the particle samples anharmonicity in the potential [18], although we note these are also observable in our data.

The optomechanical cooling of levitated nanoparticles [19,20], with the aim of attaining the quantum regime, has been the subject of several recent theoretical [21–25] and experimental [16,26–30] studies, offering an unparalleled degree of isolation from environmental noise and decoherence. There has been much success cooling nanoparticles with active feedback [26–28], while cavity red-sideband cooling has been hindered by particle-loss processes which prevented optical trapping at low background gas pressures $P \lesssim 1$ mBar [25,30,31]. However, the rich arena of two-way dynamics, from strong coupling to the quantum field of the cavity [1], is unique to cavity-cooled setups, and so motivated intense interest in finding a solution [16,29,30]. This “bottleneck” was overcome [16] via the use of a hybrid electro-optical trap, allowing trapping for up to 0.3 s, although G_1 was too weak to permit a detectable modulation of the cavity field.

However the setup reported here, with a 20-fold increase in G_1 , now allows for trapping for indefinite periods, at ultrahigh vacuum, limited only by our current equipment $\sim 10^{-6}$ mbar and unaided by feedback or any stabilization method (which introduce additional sources of noise and

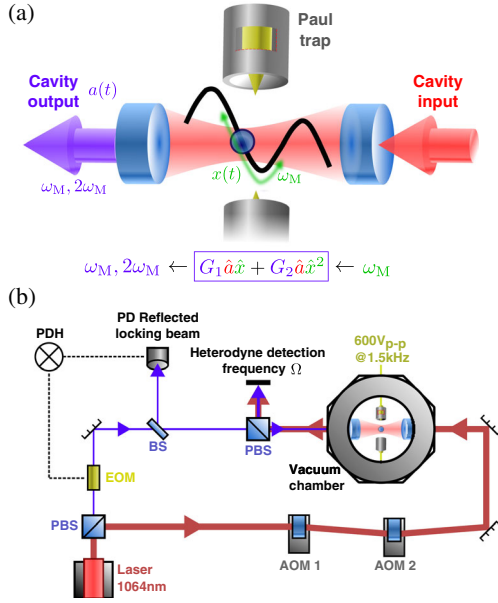


FIG. 1. Concept and experiment. (a) A particle trapped in an optical well of the hybrid trap oscillates at mechanical frequency ω_M . The cavity output is modulated by linear and quadratic coupling terms of variable strength. (b) A single laser beam is split into two beams. One is passed through an electro-optic modulator (EOM) to provide sidebands for a Pound-Drever-Hall locking scheme that locks the laser to the cavity resonance. The second beam, which drives the cooling or trapping, passes through two acousto-optic modulators (AOMs) to provide a beam with a tunable downshifted frequency (Δ) of up to 200 kHz to the on-resonance beam. Interference between these two beams produces a heterodyne signal that is recorded on a photodiode and centered at a frequency $\Omega = -\Delta$.

heating). Cooling rates (proportional to G_1^2) are far stronger; importantly, nontrivial coupled dynamics is evidenced by detectable modulations of the cavity field by both G_1 and G_2 contributions. We identify a previously unobserved shift of the Paul-trap secular frequencies due to the optical cavity (see also [32]), which enables readout of key parameters, such as the nanoparticle charge and mean number of photons in the cavity.

The hybrid trap consisting of an optical cavity field overlapped by a Paul trap, as illustrated in Fig. 1, is described as follows. The Paul-trap potential for a nanosphere is approximated by $V(x, y, z, t) = \frac{1}{2}m\omega_T^2(x^2 + y^2 - 2z^2) \sin(\omega_d t)$, where m is the mass of the nanosphere and $\omega_T^2 = 2QV_0/mr_0^2$, with Q the charge on the nanosphere, $\omega_d = 2\pi \times 1500$ Hz the drive frequency, $V_0 = 300$ V the amplitude of the applied voltage, and $r_0 = 0.5$ mm a parameter setting the scale of the trap potential. This potential is overlapped with the optical cavity potential given by $V_{\text{opt}}(x, y, z) = \hbar A |\bar{\alpha}|^2 \cos^2 kx e^{-2(y^2+z^2)/w^2}$, where $|\bar{\alpha}|^2 \equiv n$ is the mean intracavity photon number and the coupling strength $A = (3V_s/2V_m)[(\epsilon_r - 1)/(\epsilon_r + 2)]\omega_l$ depends on the sphere volume V_s , the mode volume $V_m = \pi w^2 L$ (with $w = 60$ μm the waist of the cavity field and $L = 13$ mm the

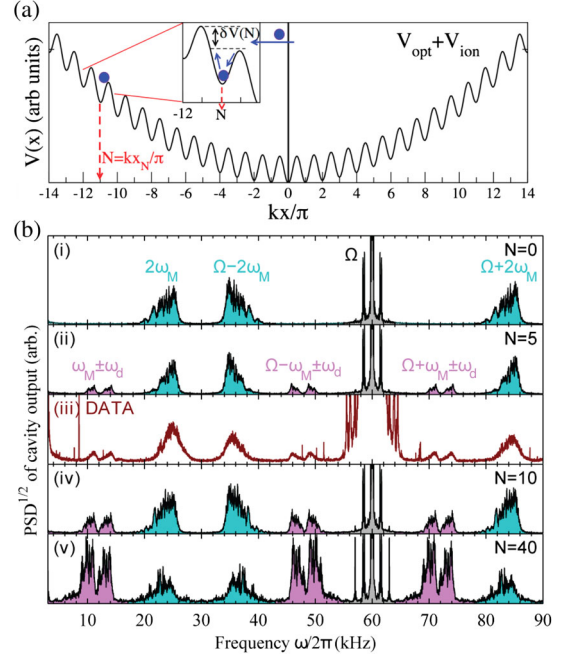


FIG. 2. (a) The hybrid-trap potential combines the Paul-trap potential with the standing-wave potential of the cavity mode. The relative strength of the optomechanical couplings (the $G_1 : G_2$ ratio) depends strongly on N , the optical well the particle becomes trapped in. (b) Comparison between simulations of the nonlinear stochastic dynamics [(i), (ii), (iv), (vi)] and an experimental spectrum, showing the latter corresponds to trapping in low $N \approx 5$ [(iii)]. $\sqrt{\text{PSD}}$ of the steady-state heterodyne spectra are shown on a linear scale. All spectra show the strong beat frequency component at $\omega = \Omega/2\pi = 60$ kHz, which is the detuning between the on-resonance locking beam and the red detuned cooling beam. The mechanical motion can be observed as sidebands around this peak at $\omega = \Omega \pm \omega_M$ due to G_1 coupling and at $\Omega \pm 2\omega_M$ due to G_2 coupling. There are also peaks at ω_M and $2\omega_M$ due to direct modulation in cavity transmission of the particle. $P = 10^{-2}$ mBar, input power $P_{\text{in}} = 0.07$ mW, $\omega_T \approx 2\pi \times 513$ Hz.

length of the cavity), and the laser frequency ω_l . This combined potential is illustrated in Fig. 2(a), and shows a particle trapped at optical well N . We set the coordinate origin to $x_N = N\pi/k$, with $\lambda = 2\pi/k = 1064$ nm.

The evolution of the axial displacement x and optical field a , in response to the motion of the particle in the two potentials, is given by

$$\begin{aligned} \ddot{x} &= \mathcal{W}|a(t)|^2 \sin(2kx) \mathcal{F}(y, z) - \gamma_M \dot{x} - \omega_T^2 x \sin(\omega_d t) + \zeta_x(t), \\ \dot{a} &= i\Delta a - i\mathcal{E} + iA a \cos^2(kx) \mathcal{F}(y, z) - \frac{\kappa}{2} a + \eta(t), \end{aligned} \quad (1)$$

where $\Delta = \omega_l - \omega_c < 0$ is the detuning of the cooling laser from the cavity resonant frequency ω_c , \mathcal{E} is its amplitude, and κ is the cavity decay rate. $\mathcal{F}(y, z)$ is the envelope of the optical field, $\mathcal{W} = -\hbar k A / m$, $\eta(t)$, $\zeta_x(t)$ are stochastic terms, and γ_M is the damping due to background gas. The $\zeta_x(t)$ terms arise from the background bath of gas at room

temperature with $\langle \zeta_x(t')\zeta_x(t) \rangle \approx 2\gamma_M(k_B T/m)\delta(t-t')$, where $T_B = 300$ K and $\eta(t)$ is the photon shot noise. For simplicity, here we analyze only the axial motion, but the full 3D stochastic nonlinear equations were solved in our simulations, with $\gamma_M \approx 0.11 \times 10^4$ P s⁻¹ where the pressure P is in mBar [32].

It is useful to consider small displacements about equilibrium: we let $x(t) = \delta x(t) + x_0$, where $\delta x(t)$ are small displacements about the equilibrium position x_0 , and we let $a(t) = \bar{a} + \delta a(t)$, where $\delta a(t)$ are small amplitude fluctuations about the mean cavity field \bar{a} . The equations of motion are now given by (see [32] for further details)

$$m\ddot{\delta x} \approx -m\omega_M^2 \delta x - \hbar(\delta a + \delta a^*)(G_1 + 2xG_2) - \gamma_M \dot{\delta x},$$

$$(\dot{\delta a}) \approx i\Delta^{x_0} \delta a - i[G_1 \delta x + G_2(\delta x)^2] - \frac{\kappa}{2} \delta a, \quad (2)$$

where $m\omega_M^2 = 2\hbar k^2 A |\bar{a}|^2 \cos(2kx_0)$ $\mathcal{F}(y, z) \approx 1$ and $\Delta^{x_0} = \Delta + A \cos^2 kx_0$. The position-dependent linear and nonlinear couplings are given by $G_1 = kA\bar{a} \sin(2kx_0)$ and $G_2 = k^2 A \bar{a} \cos(2kx_0)$.

The effect of the oscillating Paul-trap field is to force a periodic excursion of the equilibrium point x_0 ,

$$\sin 2kx_0(t) \approx -\frac{\omega_T^2}{\omega_M^2} 2\pi N \sin(\omega_d t), \quad (3)$$

with a period which is slow compared with the mechanical oscillations because $\omega_M \gg \omega_d$. The amplitude of this oscillation depends on N and this excursion is essential for effective cooling, with a rate

$$\Gamma_{\text{opt}} \approx \overline{G_1^2} \kappa [S(\omega_M) - S(-\omega_M)], \quad (4)$$

where $S(\omega) = [(\Delta^{x_0} - \omega)^2 + (\kappa/2)^2]^{-1}$ and period-averaged coupling $\overline{G_1^2} \approx (\chi/2)nN^2$ where $n = |\bar{a}|^2$ and $\chi = (\omega_T^4/\Omega_M^4)4\pi^2 k^2 A^2$. Thus if $x_0 = 0$, then $G_1 = 0$ and there is no cooling, but G_2 is maximal.

A schematic diagram of the hybrid electro-optical trap is shown in Fig. 1(a). It consists of an optical cavity [finesse $F \approx 50000$, where $\kappa \approx \pi c/(FL)$], integrated within a Paul trap inside a vacuum chamber. The Paul trap is formed by two electrodes that are perpendicular to the cavity axis. Silica nanospheres of radius 209 nm (typically with a few elementary charges [32]) can be stably trapped in the absence of the optical field. Nanospheres are introduced into the hybrid trap by initially placing them on an oscillating piezo-disk speaker. Light from a solid-state 1064-nm laser is split into a weak and a strong beam formed by a 90:10 beam splitter (BS), as illustrated in Fig. 1(b). The weaker beam is used to keep the laser locked to the cavity, via the Pound-Drever-Hall method, while the stronger beam is used for trapping and cavity cooling. Its frequency can be shifted with respect to the

cavity resonance by using two cascaded acousto-optic modulators.

We trap a particle initially at a pressure of 0.1–0.5 mBar. Once trapped, the particle stays permanently localized on a cavity antinode as the pressure is reduced to the current limit of our chamber at approximately 10^{-6} mBar. The mechanical frequency of the particle ($\omega_M = 2\pi \times 10\text{--}40$ kHz in our experiments) can be observed from the heterodyne spectrum of the recorded time series after the particle is trapped. As the transmitted cooling light from the cavity (red detuned by $-\Delta/2\pi = 50\text{--}100$ kHz) is heterodyned with the on-resonance weak beam reflected from the cavity a strong beat frequency at $\Omega = -\Delta$ is observed. The mechanical motion can be observed as heterodyne sidebands around this peak in the spectrum at $\Omega \pm \omega_M$ due to G_1 coupling and at $\Omega \pm 2\omega_M$ due to G_2 coupling. There are also peaks at ω_M and $2\omega_M$ due to direct modulation of cavity transmission by the particle.

These features are clearly illustrated in Fig. 2(b), which shows plots of the recorded heterodyne spectrum ($\text{PSD}^{1/2}$) for a nanoparticle captured near to the center of the optical potential. Simulations are also included, for comparison. For these low N , the nonlinear contribution evidenced by strong modulation at approximately $2\omega_M$ dominates. Experimental data corresponding to these simulations are shown in Fig. 2(c) for comparison. Here the splitting of the mechanical frequency and the sidebands by the Paul trap drive can be easily observed, as well as the broad single peak at $2\omega_M$.

Figure 3 shows experimental and simulated heterodyne spectra taken at short time periods after a particle is captured in well $N \sim 450$. These illustrate how the heterodyne spectrum changes in time as the particle cools at fixed $P = 3 \times 10^{-4}$ mBar. The heterodyne spectra are averaged over a 2.4-ms period separated in time by 0.2 ms. Although the spectral features are broadened and not fully resolved due to the millisecond duration of the time interval of the recorded time series, there is good agreement between the experiment and theory. Both cases show the $2\omega_M$ nonlinear coupling or frequency-doubled sidebands which can only be detected in the first few milliseconds as they are rapidly cooled. Cooling of the linear sidebands at ω_M occurs more slowly, over a time scale ~ 10 ms. We obtain a cooling rate of $\Gamma_{\text{opt}} \approx 400$ s⁻¹ from Eq. (4). From the standard expression $T \approx 300\text{K} \times \gamma_M / (\Gamma_{\text{opt}} + \gamma_M)$ (see, e.g., [1]), this would imply $T \approx 0.3$ K at steady state.

The system exhibits an unusual split-sideband structure, differing significantly from standard optomechanical systems, which in Fig. 2 appears as doublets, separated by $2\omega_d$. The relationship between the cavity output power spectral density (PSD) and displacement spectrum $S_{xx}(\omega) = \langle |x(\omega)|^2 \rangle$ has been investigated theoretically in [34]: the characteristic signature of high $N \approx 300\text{--}600$ capture is the gradual suppression of the $\omega_M + \omega_d$ peak, resulting in a single dominant peak.

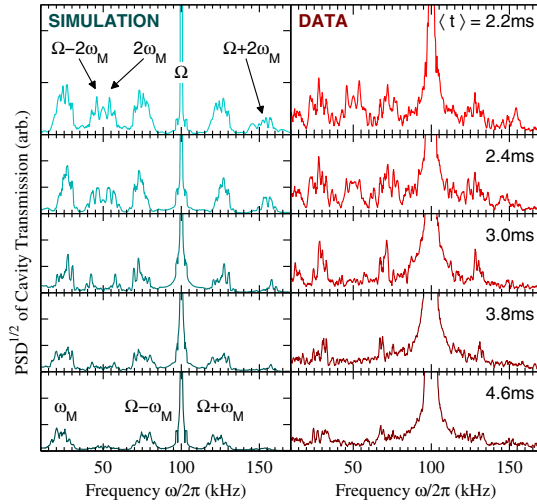


FIG. 3. Cooling dynamics of a particle which is first captured in a high ($N \approx 450$) well. From steady state, it is perturbed so that its cooling and reequilibration may be observed. The (expected) much faster damping of the G_2 sidebands at $\omega = 2\omega_M$, $\Omega \pm \omega_M$ relative to the G_1 sidebands at ω_M , $\Omega \pm \omega_M$ is clearly seen. Both experimental data and nonlinear stochastic simulations show reductions in G_1 sideband heights, which indicate cooling on ms time scales and, hence, $\Gamma_{\text{opt}} \sim 1000 \text{ s}^{-1}$. $\sqrt{\text{PSD}}$ of heterodyne spectra are shown on a linear scale. $P = 3 \times 10^{-4} \text{ mBar}$, $P_{\text{in}} = 0.5 \text{ mW}$, and $Q = 1$ [see Fig. 4(b)]. We set $\Omega = -\Delta = 2\pi \times 100 \text{ kHz}$. From these values and Eq. (4) we obtain $\Gamma_{\text{opt}} \approx 400 \text{ s}^{-1}$, in broad agreement with the observed ms cooling timescales.

The high cooling rate at high N yields low temperatures in our experiments when the pressure is reduced to the current limit of our apparatus. Such strong cooling is evidenced in the steady-state heterodyne spectra shown in Fig. 4(a). Each PSD is an average of 15 sets of 1-s duration data and are smoothed over 100 Hz. Also shown is a PSD without a trapped particle which shows the noise floor of the measurements. Here the PSD of the heterodyne detected cavity output, $S_{\text{het}}(\omega)$, for each pressure, has been calibrated assuming that at the highest pressure ($5.4 \times 10^{-1} \text{ mbar}$) there is little cooling and the nanoparticle temperature equilibrates to the surrounding gas at room temperature. Assuming also $k_B T / m\omega_M^2 = \int_{SB} S_{xx}(\omega) d\omega = C \int_{SB} S_{\text{het}}(\omega) d\omega$ and $T = 300 \text{ K}$, the calibration constant C may be evaluated (where \int_{SB} denotes the integrated area under the sidebands). Because of the relatively high background noise, the steady-state sidebands can only be clearly observed down to $P \gtrsim 10^{-4} \text{ mBar}$ even though we can clearly image the scattered light from the trapped particle on a CCD camera at 10^{-6} mBar . At such a high N , no quadratic modulation is seen in the steady-state data or the simulations.

Figure 4(b) shows a plot of the integrated area of calibrated PSD $S_{\text{het}}(\omega)$ as a function of pressure when the noise floor shown has been subtracted from the data. As

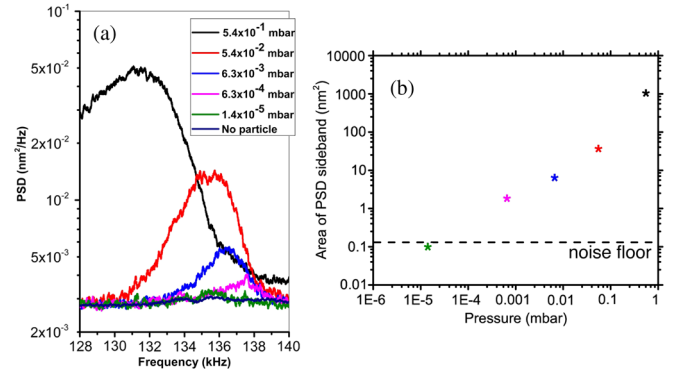


FIG. 4. (a) Steady-state data of a strongly cooled particle. The calibrated PSD spectra show single dominant peaks, indicating high N (≈ 300 – 600) trapping. Trapping occurred at a pressure $P = 0.5 \text{ mBar}$ ($T \approx 300 \text{ K}$), which was then gradually reduced to $P = 5 \times 10^{-6} \text{ mBar}$, the current limit of our apparatus. PSDs (y axes) are plotted on a log scale. Also shown is a background PSD taken with no particle trapped. The peak heights and, hence, T^{-1} scale approximately with P (see [32] for details). For $P \lesssim 10^{-5} \text{ mBar}$ it is no longer possible to detect the motional sidebands, although it can be observed from the scattered light that the particle is still trapped. $F = 50000$ and $P_{\text{in}} = 0.6 \text{ mW}$; for $N \approx 300$, Eq. (4) predicts $\Gamma_{\text{opt}} \approx 2000 \text{ s}^{-1}$. (b) Change in area of the PSD as a function of pressure demonstrating that we can measure a 1000-fold reduction in the area and, thus, the temperature limited by the noise floor of the measurement.

the area is proportional to the temperature, we demonstrate that we can measure a change in area, and thus temperature, by at least 1000 limited by the noise floor of the system. We note that although the particle remains trapped at pressures below this value with the current detection system, we cannot observe the sidebands.

In conclusion, we have investigated the effects of tunable linear G_1 and quadratic G_2 couplings in the cavity field dynamics, using both temporal behavior and steady-state spectra. Additionally, we have shown how cooling rates can be enhanced by trapping away from the Paul-trap center (at high N) where the particle is drawn away from the center of the antinode of the optical potential. Although quadratic couplings in principle offer the prospect of QND measurement of energy, this is hampered by the modest one-photon coupling strengths [32] in this system. However, the very high- Q and long coherence times offered by levitated systems may permit the realization of a scheme for detection of quantum phonon noise in [10]. We have demonstrated two-way linear and nonlinearly coupled dynamics between a cavity mode and a nanoparticle, and stable cooling and trapping at high vacuum without any additional stabilization. Cooling rates in the 1000 s^{-1} range were measured, and a factor of 100 increase is possible, with a higher finesse cavity (allowing for sideband resolved, maximal cooling) and higher input power (leading to both higher cooling and higher ω_M). This scheme could allow cooling to the ground state at pressures

below 10^{-7} mbar, which would be detectable with sensitive balanced homodyne detection.

The authors acknowledge funding from EPSRC Grant No. EP/H050434/1. E. B. A. acknowledges a Ph.D. scholarship from the Schlumberger Faculty For the Future program.

*Corresponding author.
p.barker@ucl.ac.uk

- [1] M. Aspelmeyer, T. J. Kippenberg, and F. Marquardt, *Rev. Mod. Phys.* **86**, 1391 (2014).
- [2] J. D. Teufel, T. Donner, D. Li, J. H. Harlow, M. S. Allman, K. Cicak, A. J. Sirois, J. D. Whittaker, K. W. Lehnert, and R. W. Simmonds, *Nature (London)* **475**, 359 (2011).
- [3] J. Chan, T. P. Mayer Alegre, A. H. Safavi-Naeini, J. T. Hill, A. Krause, S. Groeblacher, M. Aspelmeyer, and O. Painter, *Nature (London)* **478**, 89 (2011).
- [4] S. Weis, R. Riviere, S. Deleglise, E. Gavartin, O. Arcizet, A. Schliesser, and T. J. Kippenberg, *Science* **330**, 1520 (2010).
- [5] A. H. Safavi-Naeini and O. Painter, *New J. Phys.* **13**, 013017 (2011).
- [6] J. Bochmann, A. Vainsencher, D. D. Awschalom, and A. N. Cleland, *Nat. Phys.* **9**, 712 (2013).
- [7] R. W. Andrews, R. W. Peterson, R. W. Purdy, K. Cicak, R. W. Simmonds, C. A. Regal, and K. W. Lehnert, *Nat. Phys.* **10**, 321 (2014).
- [8] A. H. Safavi-Naeini, S. Grblacher, J. T. Hill, J. Chan, M. Aspelmeyer, and O. Painter, *Nature (London)* **500**, 185 (2013).
- [9] J. D. Thompson, B. M. Zwickl, A. M. Jayich, F. Marquardt, S. M. Girvin, and J. G. E. Harris, *Nature (London)* **452**, 72 (2008).
- [10] A. A. Clerk, F. Marquardt, and J. G. E. Harris, *Phys. Rev. Lett.* **104**, 213603 (2010).
- [11] A. Nunnenkamp, K. Borkje, J. G. E. Harris, and S. M. Girvin, *Phys. Rev. A* **82**, 021806(R) (2010); K. Borkje, A. Nunnenkamp, J. D. Teufel, and S. M. Girvin, *Phys. Rev. Lett.* **111**, 053603 (2013).
- [12] A. Kronwald and F. Marquardt, *Phys. Rev. Lett.* **111**, 133601 (2013).
- [13] K. Jacobs, L. Tian, and J. Finn, *Phys. Rev. Lett.* **102**, 057208 (2009).
- [14] C. Doolin, B. D. Hauer, P. H. Kim, A. J. R. MacDonald, H. Ramp, and J. P. Davis, *Phys. Rev. A* **89**, 053838 (2014).
- [15] D. Lee, M. Underwood, D. Mason, A. B. Shkarin, S. W. Hoch, and J. G. E. Harris, *Nat. Commun.* **6**, 6232 (2015).
- [16] J. Millen, P. Z. G. Fonseca, T. Mavrogordatos, T. S. Monteiro, and P. F. Barker, *Phys. Rev. Lett.* **114**, 123602 (2015).
- [17] G. A. Brawley, M. R. Vanner, P. E. Larsen, S. Schmid, A. Boisen, and W. P. Bowen, *Nat. Commun.* **7**, 10988 (2015).
- [18] J. Gieseler, L. Novotny, and R. Quidant, *Nat. Phys.* **9**, 806 (2013).
- [19] Z.-q. Yin, A. A. Geraci, and T. Li, *Int. J. Mod. Phys. B* **27**, 1330018 (2013).
- [20] L. P. Neukirch and A. N. Vamivakas, *Contemp. Phys.* **56**, 48 (2015).
- [21] O. Romero-Isart, M. L. Juan, R. Quidant, and J. I. Cirac, *New J. Phys.* **12**, 033015 (2010).
- [22] D. E. Chang, C. A. Regal, S. B. Papp, D. J. Wilson, J. Ye, O. Painter, H. J. Kimble, and P. Zoller, *Proc. Natl. Acad. Sci. U.S.A.* **107**, 1005 (2010).
- [23] P. F. Barker and M. N. Shneider, *Phys. Rev. A* **81**, 023826 (2010).
- [24] G. A. T. Pender, P. F. Barker, F. Marquardt, J. Millen, and T. S. Monteiro, *Phys. Rev. A* **85**, 021802 (2012).
- [25] T. S. Monteiro, J. Millen, G. A. T. Pender, F. Marquardt, D. Chang, and P. F. Barker, *New J. Phys.* **15**, 015001 (2013).
- [26] T. Li, S. Kheifets, and M. G. Raizen, *Nat. Phys.* **7**, 527 (2011).
- [27] J. Gieseler, B. Deutsch, R. Quidant, and L. Novotny, *Phys. Rev. Lett.* **109**, 103603 (2012).
- [28] B. Rodenburg, L. P. Neukirch, A. N. Vamivakas, and M. Bhattacharya, *Optica* **3**, 318 (2016).
- [29] P. Asenbaum, S. Kuhn, S. Nimmrichter, U. Sezer, and M. Arndt, *Nat. Commun.* **4**, 2743 (2013).
- [30] N. Kiesel, F. Blaser, U. Delić, D. Grass, R. Kaltenbaek, and M. Aspelmeyer, *Proc. Natl. Acad. Sci. U.S.A.* **110**, 14180 (2013).
- [31] J. Millen, T. Deesuwan, P. Barker, and J. Anders, *Nat. Nanotechnol.* **9**, 425 (2014).
- [32] See Supplemental Material at <http://link.aps.org/supplemental/10.1103/PhysRevLett.117.173602>, which includes Ref. [33], for description of cooling in the hybrid trap and characterization of the trapped particle motion.
- [33] R. E. March, *J. Mass Spectrom.* **32**, 351 (1997).
- [34] E. B. Aranas, P. G. Z. Fonseca, P. F. Barker, and T. S. Monteiro, [arXiv:1606.07377](https://arxiv.org/abs/1606.07377).